VII International Conference on Computational Methods for Coupled Problems in Science and Engineering
COUPLED PROBLEMS 2017
M. Papadrakakis, E. Oñate and B. Schrefler (Eds)

NUMERICAL MODELLING OF COUPLED THERMO-HYDRAULIC PROBLEMS FOR LONG-TERM GEOTHERMAL RESERVOIR PRODUCTIVITY

Hua-Peng Chen[1*] and Musa D. Aliyu[1]

[1]Department of Engineering Science, University of Greenwich, Medway Campus, Kent, UK
*Corresponding author: H.Chen@greenwich.ac.uk
M.D.Aliyu@greenwich.ac.uk

Key words: Geothermal energy extraction, coupled thermo-hydraulic, finite element method, multiple phase, productivity simulations.

ABSTRACT

The advent of geothermal energy has opened a new chapter in global energy demand, for clean, renewable, and sustainable sources. This energy form is harnessed by creating a reservoir in a formation that serves as a heat exchanger. Modelling provides a means of representing concepts and approaches in reservoir simulation. Several methods are proposed to simulate geothermal reservoir behaviour under long-term performance, but it is very hard to specify the most powerful and realistic approach in forecasting reservoir lifespan. The aim of this work is to evaluate two different approaches: equivalent porous media (EPM) and dual porosity-permeability (DPP) model, for simulating geothermal reservoir long-term performance and to assess the adequacy of these approaches. The finite element method is employed to develop and simulate the numerical models based on the two different approaches in forecasting the productivities of the reservoirs during exploitation period of 30 years. The parameters investigated are the temperature, density, and viscosity distribution under the influence of coupled thermal and hydraulic processes. The simulation results are analysed and compared with the different approaches using those parameters. The analysis indicates that both the approaches can efficiently estimate the long-term performance of a reservoir to some extent, but further investigations are required regarding the effect of other coupling terms.

1. INTRODUCTION

The transport of fluid and heat through naturally fractured reservoirs is a method that holds importance for many fields of geosciences, ranging from geothermal mining to oil and gas. Studies on fluid and heat transport in naturally fractured reservoirs have a history that spans nearly six decades[1]. Numerous conceptual models have been developed for representing fluid and heat flow in naturally fractured reservoirs, and each model can be differentiated from the other by transport capabilities and storage of the fracture and the porous medium. Thus, the transport characteristics are associated with permeability, and the storage characteristics are related to porosity [2]. It is imperative to consider the various modelling approaches available for simulating heat and fluid flow in naturally fractured reservoirs and understanding the advantages and limitations of each approach.

Since the 1960's, the numerical modelling of naturally fractured reservoirs using dual porosity-permeability models has been the subject of many studies. The modelling approach has been accepted and implemented in different fields of reservoir engineering. For instance, several authors [3]–[8] have developed simulation code applying different techniques using the dual porosity model. On the other hand, the equivalent porous media model is also widely employed in modelling naturally fractured reservoirs, but this is not as common as the former model. Numerous researchers [9]–[13] have used the equivalent porous media approach for modelling different categories of reservoirs. Despite the dissimilarities in modelling assumptions, it appears that no studies have tried to compare the outcomes of those models and determine if they are acceptable. It is evident that additional study is required to better quantify these modelling approaches with the help of valid comparisons.

The objectives of this investigation are to compare two different approaches for fluid and heat transport in a naturally fractured geothermal reservoir; in this case, the dual porosity-permeability (DPP) model and the equivalent porous media (EPM) model. The two models are based on the conservation of mass for flow and the conservation of energy for heat transport in order to evaluate the ability of both models to simulate heat and fluid flow in a naturally fractured geothermal reservoir and assess the advantages and limitations of each model.

2. MODELLING FLUID AND HEAT TRANSPORT IN A FRACTURED RESERVOIR

In this study, the heat and fluid transport analyses in a naturally fractured reservoir are modelled using two alternative approaches: the DPP model and the EPM model. The two approaches are briefly described in this section.

2.1 Equivalent porous media (EPM) model

In the EPM model for naturally fractured systems, the initial assumption is that fracture behaviour is equivalent to porous media for both heat and fluid transport. The modelling approach assumes that an equivalent porous medium can represent the matrix block including fractures with equivalent conductivity in a particular area. It approximates the overall local conductivity of the fractures as well as the matrix with an improved equivalent conductivity [9]. Thus, the continuity equation expressing the conservation of mass in a fully saturated porous medium can be expressed as

$$\phi \frac{\partial \rho_L}{\partial t} + \nabla \cdot (\rho_L v) = 0 \tag{1}$$

where ϕ is the porosity, ρ_L is the fluid density, and v is the Darcy's velocity. The momentum conservation is expressed by Darcy's law

$$v = -\frac{\kappa}{\mu}(\nabla P - \rho_L g \nabla z) \tag{2}$$

in which κ is the hydraulic permeability, μ is the fluid dynamic viscosity, P is the hydraulic pressure, g is the acceleration due to gravity, and z is the vertical depth.

$$(\rho C_P)\frac{\partial T}{\partial t}+\nabla\cdot(\rho_L C_{P,L} vT)-\nabla\cdot(\lambda\nabla T)=0 \tag{3}$$

where T is the temperature, $C_{P,L}$ is the fluid heat capacity, ρC_P is the effective densities and heat capacities of the saturated porous medium, and λ is the effective thermal conductivities. The last two terms are expressed as

$$\rho C_P=(1-\phi)\rho_S C_{P,S}+\phi\rho_L C_{P,L} \tag{4}$$

$$\lambda=(1-\phi)\lambda_S+\phi\lambda_L \tag{5}$$

in which ρ_S is the solid density, $C_{P,S}$ is the solid heat capacity, λ_S and λ_L are the solid and fluid thermal conductivities, respectively. In this case, both expressions are used to represent the porous matrix and the fracture.

2.2 Dual porosity-permeability (DPP) model

In this model, the matrix and fracture system are modelled as separate but connected systems. Fluid mass transfer between the matrix block and fractures occur at the fracture-matrix interface. The approach is based on the concept that unfractured rock accounts for much of the porosity (storage) of the medium but little permeability (flow). On the other hand, fractures may have high permeability with negligible storage.

In this case, the matrix equation for both the fluid and heat transport is the same as equations (1) to (5) represented in the EPM model; therefore, it will not be repeated here. The fluid flow in fracture within a porous matrix is expressed as

$$\phi_f\frac{\partial\rho_L}{\partial t}+\nabla\cdot\rho_L v_f+Q_f+Q_m=0 \tag{6}$$

where ϕ_f is the fracture porosity, Q_m and Q_f are the fluid mass sources/sinks for the fracture and matrix, respectively. The variable v_f is the Darcy's velocity for the fracture expressed as

$$v_f=-\frac{b^2}{12\mu}(\nabla P_f-\rho_L g\nabla z) \tag{7}$$

in which b is the fracture aperture, and P_f is the fluid pressure within the fracture. For the heat transfer in fracture within a porous matrix is given as

$$\rho C_p\frac{\partial T}{\partial t}+\rho_L C_{P,L} v_f T-\nabla(\lambda\nabla T)+Q_{f,E}+Q_{m,E}=0 \tag{8}$$

where $Q_{f,E}$ is the energy sources/sinks for the fracture, and $Q_{m,E}$ is the energy sources/sinks for the porous matrix.

2.3 Coupling heat and fluid flow

The macroscopic equations presented above for both models contain the non-linear coupling between the fluid and heat transport. Heat transport depends on flow via heat convection (i.e., velocity field), as expressed in equation (5). Fluid flow depends on heat transport via the temperature dependence of the fluid density, viscosity, specific heat capacity, and thermal conductivity, as presented below from equations (9) to (12) [14].

$$\rho_L(T)=996.9\left(1-3.17\times10^{-4}(T-298.15)-2.56\times10^{-6}(T-298.15)^2\right) \tag{9}$$

$$\mu(T)=2.414\times10^{-5}\times10^{\frac{247.8}{(T+133)}} \tag{10}$$

$$\lambda_L(T)=-922.47+2839.5\left(\frac{T}{T_0}\right)-1800.7\left(\frac{T}{T_0}\right)^2+525.77\left(\frac{T}{T_0}\right)^3-73.44\left(\frac{T}{T_0}\right)^4 \tag{11}$$

$$C_{P,L}(T)=3.3774-1.12665\times10^{-2}T+1.34687\times10^{-5}T^2 \tag{12}$$

3. MODEL SET-UP AND CONFIGURATION FOR THE BASE CASE

The geothermal reservoir for the base case is assumed to consist of two wellbores (i.e., injection and production) that intersect a fracture within the reservoir domain. Figure 1 shows the geometry of the base case. It represents a three-dimensional (3-D) deep geothermal reservoir with the dimensions 500 m x 500 m x -5050 m, with a thickness of 500 m, and located at about -4550 m below the ground level. The wellbores constitute a doublet, 11 m apart at the ground level, and 400 m apart laterally at the fracture intersection level.

In this study, the fracture is modelled in two different forms. For the EPM model, the fracture is considered as a 3-D domain. In the case of the DPP model, the fracture is represented as a plane surface with thickness.

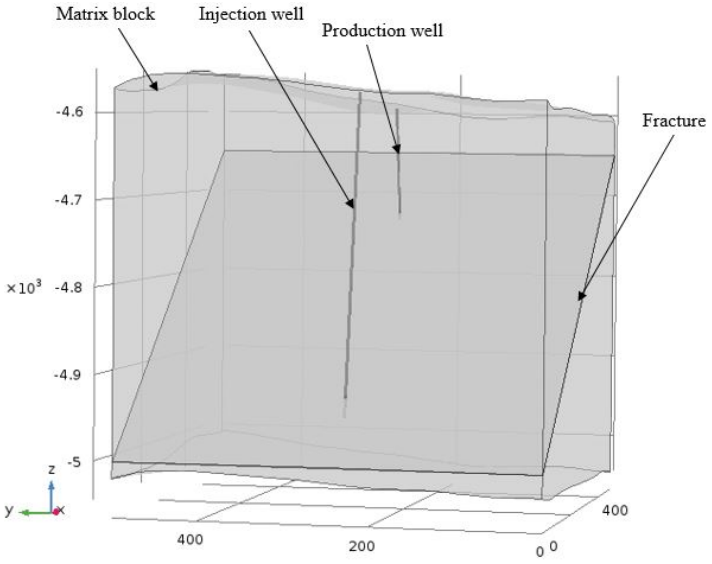

Figure 1: Reservoir geometry

3.1 Initial and boundary conditions

Initially, at t=0, the pressure is hydrostatic, and the temperature is assumed to be

$$T_0 = 12°C - 38°C(K/m)(-z) \tag{13}$$

where T_0 is the initial reservoir temperature. For hydraulic boundary conditions (B.C) a constant injection pressure of 10 MPa is applied. In the case of the thermal B.C an injection temperature of 40°C is employed at the injection wellbore. All other boundaries remain thermally insulated and no flow for the conditions for both the heat and fluid models, respectively. Table 1 presents the material properties employed in the numerical modelling.

Table 1: Physical properties attributed to base case reservoir [8]

Parameter	Value	Symbol
Matrix		
Porosity (%)	0.6	ϕ
Permeability (mD)	0.01	κ
Thermal conductivity (W/m/K)	3.5	λ_s
Heat capacity (J/kg/K)	900	$C_{\rho,S}$
Density (kg/m^3)	2400	ρ_s
Fracture		
Porosity (%)	0.1	ϕ_f
Permeability (mD)	10	κ_f
Thermal conductivity (W/m/K)	2.5	λ_f
Heat capacity (J/kg/K)	750	$C_{\rho,f}$
Density (kg/m^3)	1200	ρ_f

3.2 Computational cost and performance

In order to compare the computational cost and performance for the EPM and DPP models, a backwards difference formula (BDF) is used in the finite element solver to run the long-term simulation for 30 years. For the EPM model, it took 50-time steps with a simulation period of 29,278 seconds to simulate the 30-year numerical experimentation. The physical memory utilised is 14.98 GB, and the virtual memory is 17.26 GB. However, in the case of DPP model, it only took 33 time steps with a solution period of 307 seconds to solve for the entire process. Concerning the physical memory and virtual memory, 2.26 GB and 2.39 GB were applied, respectively.

Thus, the percentage deviation between the two models is 195.85% in terms of simulation time, 147.58% with respect to physical memory, and 151.35% in regards to virtual memory. It is also worth noting that to solve for one model using EPM is equivalent to solving 95 models in DPP.

4. RESULTS AND DISCUSSIONS

Figure 2 shows the temperature breakthrough curves obtained with both the EPM and DPP models for the same base case. Comparison of the two models, EPM and DPP, for the base case shows that very similar breakthrough curves are produced during the first seven years of the simulation. After approximately 7.2 years, the results concerning reservoir productivity, obtained with the EPM model, are slightly better than the one obtained with the DPP model. However, the calculated equivalent porosity and permeability models for the EPM model are extremely high and not realistic, if compared to the simulation domain dimensions. Table 2 presents the percentage deviation between the EPM and DPP models. As can be seen, there is more fitting for both models in the first seven years of production. For the later production period, a drastic drawdown is observed with the DPP model and a maximum deviation of 2.2% is reached between the two models in 30 years.

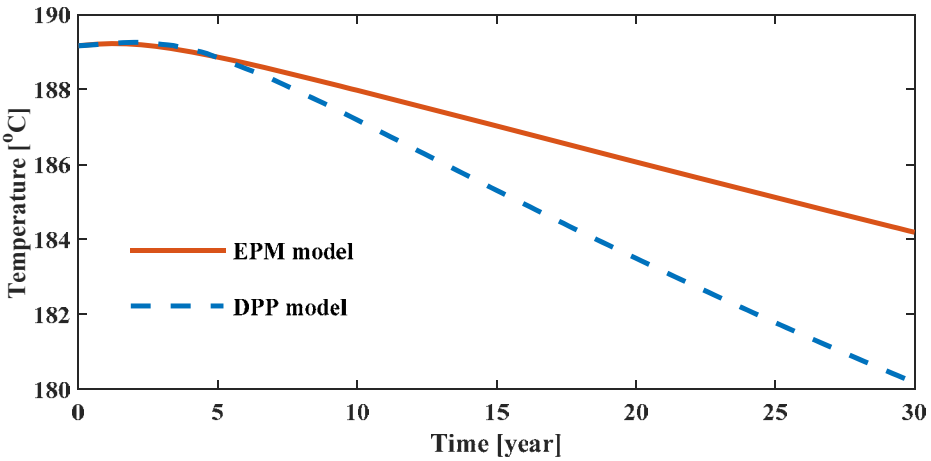

Figure 2: Temperature at the production wellbore for both EPM and DPP models

Table 2: Percentage deviation for the production temperature between the EPM and DPP models

Time (year)	EPM model production temperature (°C)	DPP model production temperature (°C)	Percentage deviation (%)
1	189.22	189.22	0
5	188.86	188.85	0.005
10	187.98	187.19	0.421
15	187.03	185.31	0.924
20	186.07	183.50	1.391
25	185.12	181.78	1.821
30	184.19	180.18	2.201

The density at the production wellbore for both the EPM and DPP models was shown in Figure 3 during a long-term simulation period of 30 years. As demonstrated in Figure 3, the production temperature remains unchanged as seen from the first five years of the simulation for both models. However, if the production temperature decreases, the density rises rapidly due

specifically to its dependence on temperature. In this scenario, the density of the DPP model is higher on the producer than that of the EPM because the EPM model has a higher production temperature. Similarly, Figure 4 presents the viscosity variation with time at the production wellbore for both the models. As can be seen, the case is exactly the same as the density since both properties are temperature-dependant parameters.

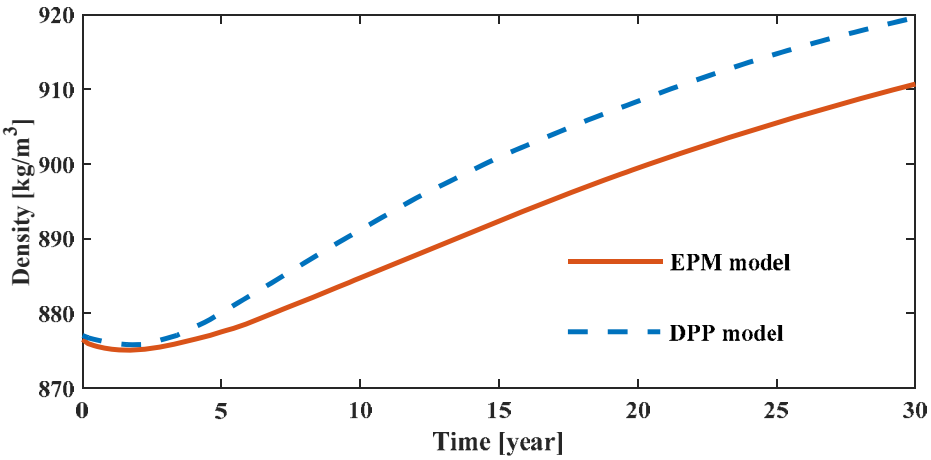

Figure 3: Density at the production wellbore for both EPM and DPP models

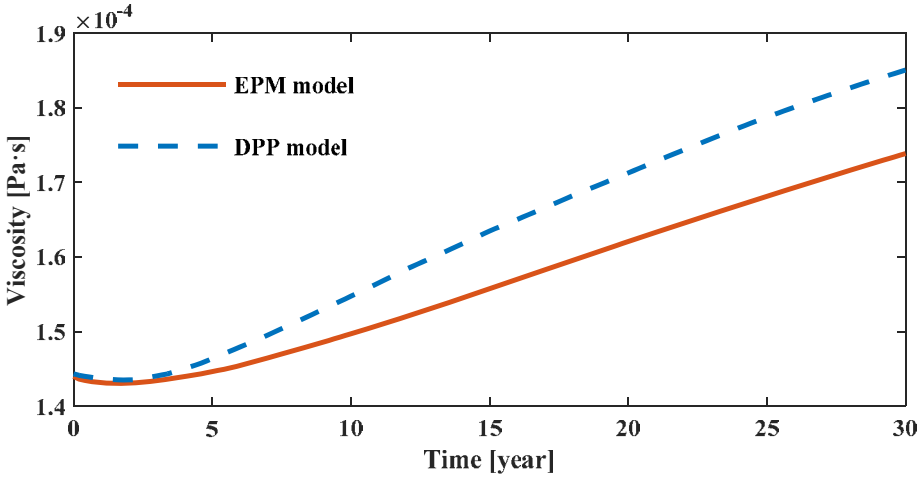

Figure 4: Density at the production wellbore for both EPM and DPP models

Figures 5a-d shows the evolution of the cold water front in the fracture surface at some simulation stages for both the EPM and DPP models. The low-temperature areas are highlighted using the legends with lower and higher threshold values 40°C and 200°C, respectively, indicating the inability of the surface to produce effective temperatures further. Since the exploitation began, the cold water front region in the fracture surface grew gradually from the injection wellbore in an annular shape for both models as shown in Figures 5a-d. As can be seen, the cold water front propagation trends are similar in both the EPM and DPP models, despite the differences in their modelling approaches.

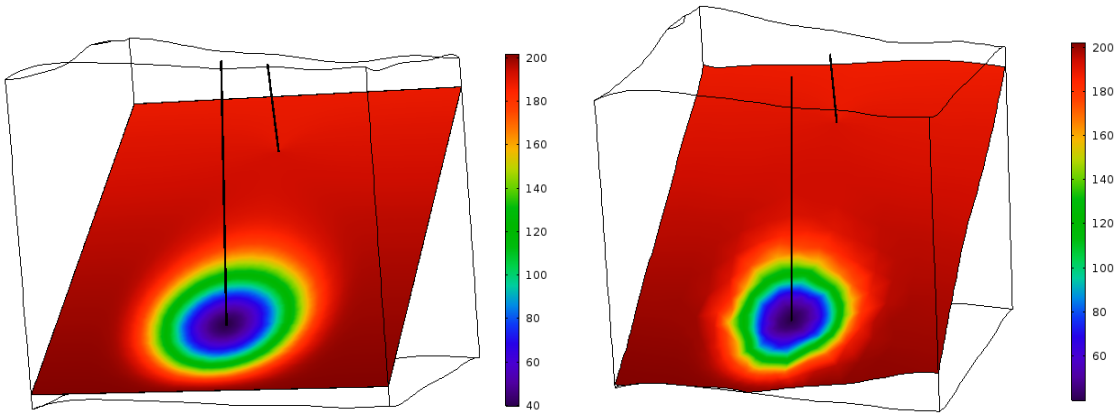

Figure 5a: EPM model at 1-year simulation (left); and DPP model at 1-year simulation (right) [°C]

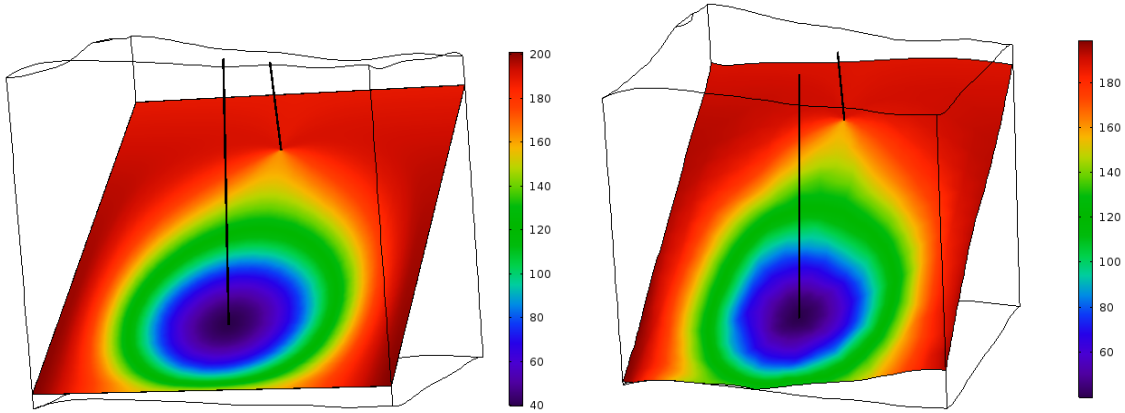

Figure 5b: EPM model at 10-years simulation (left); and DPP model at 10-years simulation (right) [°C]

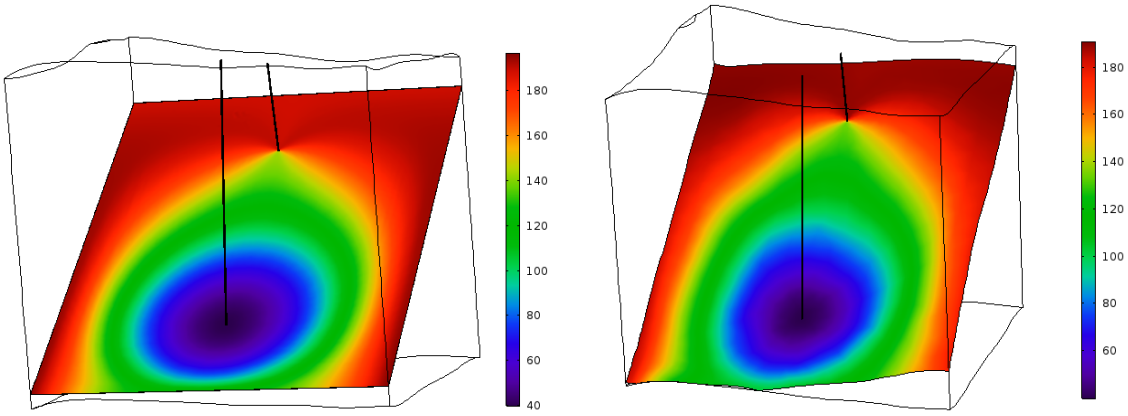

Figure 5c: EPM model at 20-years simulation (left); and DPP model at 20-years simulation (right) [°C]

Figure 5: EPM (left), and DPP (right) models cold water front at fracture surface at various simulation stages [°C]

5. CONCLUSION

This paper compared two modelling approaches, EPM and DPP conceptual models, of a naturally fractured geothermal reservoir using the finite element method to predict the long-term performance of coupled transient processes of heat and fluid transport. Two deep 3-D numerical models of doublet geothermal reservoirs are developed with the same material properties as a base case for the two models to carry a comparative study. The production temperature, density, and viscosity are examined and compared to both the EPM and DPP models during a long-term simulation period of 30 years. Besides, the cold water front evolution has been evaluated at several simulation stages for the models. The simulations show that the two models could be equally well-modelled heat and fluid flow in a naturally fractured geothermal reservoir with negligible errors. Based on the results obtained, the current work suggests that EPM and DPP models can be used for predictions, which are needed for decision making for several subsurface related issues, such as hydrocarbon reservoirs, waste disposal reservoirs, and carbon dioxide (CO_2) sequestration reservoirs.

REFERENCE

[1] M. J. O'Sullivan, K. Pruess, and M. J. Lippmann, "State of the art of geothermal reservoir simulation," *Geothermics*, vol. 30, no. 4, pp. 395–429, Aug. 2001.

[2] J. Willis-Richards and T. Wallroth, "Approaches to the modelling of hdr reservoirs: A review," *Geothermics*, vol. 24, no. 3, pp. 307–332, Jun. 1995.

[3] O. Kolditz, "Modelling flow and heat transfer in fractured rocks: dimensional effect of matrix heat diffusion," *Geothermics*, vol. 24, no. 3, pp. 421–437, Jun. 1995.

[4] T. Kohl and R. J. Hopkirk, "'FRACure' — A simulation code for forced fluid flow and transport in fractured, porous rock," *Geothermics*, vol. 24, no. 3, pp. 333–343, Jun. 1995.

[5] O. Kolditz and C. Clauser, "Numerical simulation of flow and heat transfer in fractured crystalline rocks: Application to the Hot Dry Rock site in Rosemanowes (U.K.)," *Geothermics*, vol. 27, no. 1, pp. 1–23, Feb. 1998.

[6] M. D. Aliyu and H. Chen, "Numerical Modelling of Coupled Hydro-Thermal Processes of the Soultz Heterogeneous Geothermal System," in *ECCOMAS Congress 2016 VII European Congress on Computational Methods in Applied Sciences and Engineering M. Papadrakakis, V. Papadopoulos, G. Stefanou, V. Plevris (eds.) Crete Island, Greece, 5–10 June 2016*, 2016, no. June, pp. 1–13.

[7] M. D. Aliyu, H. Chen, and O. Harireche, "Finite element modelling for productivity of geothermal reservoirs via extraction well," in *Proceedings of the 24th UK Conference of the Association for Computational Mechanics in Engineering 31 March– 01 April 2016, Cardiff University, Cardiff*, 2016, no. April, pp. 331–334.

[8] O. Kolditz, R. Ratke, H.-J. G. Diersch, and W. Zielke, "Coupled groundwater flow and

transport: 1. Verification of variable density flow and transport models," *Adv. Water Resour.*, vol. 21, no. 1, pp. 27–46, Feb. 1998.

[9] R. Ghasemizadeh, X. Yu, C. Butscher, F. Hellweger, I. Padilla, A. Alshawabkeh, and B. Y. Cao, "Equivalent porous media (EPM) simulation of groundwater hydraulics and contaminant transport in Karst aquifers," *PLoS One*, vol. 10, no. 9, pp. 1–12, 2015.

[10] A. Ebigbo, J. Niederau, G. Marquart, I. Dini, M. Thorwart, W. Rabbel, R. Pechnig, R. Bertani, and C. Clauser, "Influence of depth, temperature, and structure of a crustal heat source on the geothermal reservoirs of Tuscany: numerical modelling and sensitivity study," *Geotherm. Energy*, vol. 4, no. 1, p. 5, 2016.

[11] T. Chen, C. Clauser, G. Marquart, K. Willbrand, and H. B??sing, "Modeling anisotropic flow and heat transport by using mimetic finite differences," *Adv. Water Resour.*, vol. 94, pp. 441–456, 2016.

[12] J. Niederau, A. Ebigbo, G. Marquart, J. Arnold, and C. Clauser, "On the impact of spatially heterogenous permeability on free convection in the Perth Basin, Australia," *Geothermics*, vol. 66, no. April, pp. 119–133, Mar. 2017.

[13] D. Blessent, P. R. Jørgensen, and R. Therrien, "Comparing Discrete Fracture and Continuum Models to Predict Contaminant Transport in Fractured Porous Media.," *Groundwater*, vol. 52, no. 1, pp. 84–95, 2013.

[14] E. O. Holzbecher, *Modeling Density-Driven Flow in Porous Media*. Berlin, Heidelberg: Springer Berlin Heidelberg, 1998.